
KGPFN: Unlocking the Potential of Knowledge Graph Foundation Model via In-Context Learning

Yisen Gao¹, Jiaxin Bai², Haoyu Huang¹, Zhongwei Xie¹, Yufei Li¹, Hong Ting Tsang¹, Sirui Han^{1*}
Yangqiu Song¹

Department of Computer Science and Engineering, HKUST, Hong Kong, China¹
Department of Computer Science and Engineering, HKBU, Hong Kong, China²

{ygaodi}@cse.ust.hk

Abstract

Knowledge graph (KG) foundation models aim to generalize across graphs with unseen entities and relations by learning transferable relational structure. However, most existing methods primarily emphasize relation-level universality, while in-context learning, the other pillar of foundation models remains under-explored for KG reasoning. In KGs, context is inherently structured and heterogeneous: effective prediction requires conditioning on the local context around the query entities as well as the global context that summarizes how a relation behaves across many instances. We propose KGPFN, a KG foundation model using Prior-data Fitted Network that unifies transferable relational regularities with inference-time in-context learning from structured context. KGPFN first learns relation representations via message passing on relation graphs to capture cross-graph relational invariances. For query-specific reasoning, it encodes local neighborhoods using a multi-layer NBFNet as local context. To enable ICL at global scale, it constructs relation-specific global context by retrieving a large set of instances of the query relation together with their local neighborhoods, and aggregates them within a Prior-Data Fitted Network framework that combines feature-level and sample-level attention. Through multi-graph pretraining on diverse KGs, KGPFN learns when to instantiate reusable patterns and when to override them using contextual evidence. Experiments on 57 KG benchmarks demonstrate that KGPFN achieves strong adaptation to previously unseen graphs through in-context learning alone, consistently outperforming competitive fine-tuned KG foundation models. Our code is available at <https://github.com/HKUST-KnowComp/KGPFN>.

1 Introduction

Foundation models have emerged as a dominant paradigm across artificial intelligence, achieving strong generalization through large-scale pretraining and inference-time adaptation via context. Large language models [32, 28, 44] demonstrate that a single pretrained model can carry out diverse tasks such as translation, summarization, question answering, information extraction, and code generation, where the task is specified by the inference-time context together with a few in-context [1, 11] input-output demonstrations. Beyond unstructured modalities, foundation models for structured data are increasingly built around the Prior-Data Fitted Network (PFN) [31] in-context learning paradigm, in which a single model acquires general-purpose predictive capabilities by training on large synthetic datasets and subsequently infers the appropriate task and schema from a small context set at inference time. This line of work includes tabular foundation models such as TabPFN [22, 19], TabICL [33, 34],

*Sirui Han is the corresponding author.

Limix [47], time-series foundation models [41], and emerging extensions to relational data [45]. Two recurring themes cut across these models: *broad transferability* across tasks and domains with minimal or no retraining, and *strong in-context learning*, namely the ability to adapt predictions by conditioning on a small set of labeled examples provided at inference time.

Knowledge graphs (KGs) are widely used to represent relational data in applications such as question answering [2, 17], recommendation [8], and drug discovery [18], and they also motivate neural graph databases that support graph management and querying with learned representations [4, 6, 35, 46, 26]. Recently, KG foundation models [16, 23, 12, 48] have been proposed to overcome key limitations of traditional KG embedding methods [3, 36, 7], which are largely transductive and require retraining from scratch for each new graph. Instead of learning graph-specific entity embeddings, KG foundation models aim to acquire transferable relational knowledge that generalizes across KGs with different entity/relation vocabularies, enabling zero-shot or few-shot adaptation to unseen graphs.

However, existing KG foundation models [16, 12, 48, 23] largely emphasize the universality of relational patterns, while paying far less attention to the second pillar of foundation models, namely in-context learning. Bringing in-context learning to knowledge graphs has therefore emerged as a central challenge for KG foundation models: models tend to over-apply broadly reusable patterns and fail to adapt their predictions to the specific graph instance at hand without in-context learning. Inspired by recent progress on structured foundation models [22, 19, 47], extending PFN-paradigm in-context learning to KG-structured data is a promising direction. Yet this extension is non-trivial. Unlike text or table data, context in knowledge graphs is inherently more structured and more heterogeneous: it is not a single surrounding window, but a combination of (i) local context: the query-specific neighborhood in which reasoning takes place and (ii) global context: the relation-specific evidence accumulated across many instances. Accordingly, KG context naturally decomposes into two complementary parts.

Local context is the immediate subgraph around the query entities. It matters because the same relation can yield different predictions depending on the surrounding neighborhood: a reusable structural cue may be reliable in one local subgraph yet misleading in another. As shown in Fig. 1 left, consider the “triangle” pattern (person, born_in, city) and (city, located_in, nation), which, for many individuals, is consistent with (person, nationality, nation). For instance, for (Demis Hassabis, born_in, London) and (London, located_in, UK), the local structure aligns with (Demis Hassabis, nationality, UK). Yet the same cue can fail in other neighborhoods, such as (Fei-Fei Li, born_in, Beijing) and (Beijing, located_in, China), where nationality is not determined by the birth-country neighborhood alone. Importantly, local neighborhoods may also include additional relations that modulate or override the birth-based cue. For example, employment edges such as (person, works_at, Stanford) or (person, works_at, DeepMind) can provide complementary signals about the appropriate prediction. Together, these examples illustrate that models must condition on local neighborhoods to decide when a generic pattern should be instantiated and when it should be overridden.

Global context captures relation-level regularities across the graph, describing how a relation behaves over many instances rather than within a single neighborhood. As shown in Fig. 1 right, for a given relation type, global context can be formed by a set of representative instances together with their associated local neighborhoods. Such a collection provides a distributional view of how the relation is typically grounded in graph structure: which auxiliary relations and multi-hop paths tend to co-occur with it, how frequently they appear, and how they constrain plausible heads and tails. In this sense, relational universality and context are complementary: universality captures what relational structure can be reused, while local and global context determine where and how that structure should be instantiated within a particular graph. Enabling large-scale in-context learning for knowledge graphs is therefore a necessary step toward truly general KG foundation models.

Based on the above analysis, we propose **KGPFN**, a model designed to unlock the potential of **Knowledge Graph** foundation model through in-context learning via **Prior-data Fitted Network**. KGPFN integrates two complementary capabilities: learning relation-general regularities and utilizing the context at inference time. Concretely, we first perform message passing over the relation graphs to obtain relation representations that capture transferable, relation-level structure. To encode local context, we apply a multi-layer NBFNet to compute neighborhood-aware vectors for the query entities. To incorporate global context, we retrieve a large set of instances that share the query relation, together with their local neighborhoods, and model them within a PFN framework that

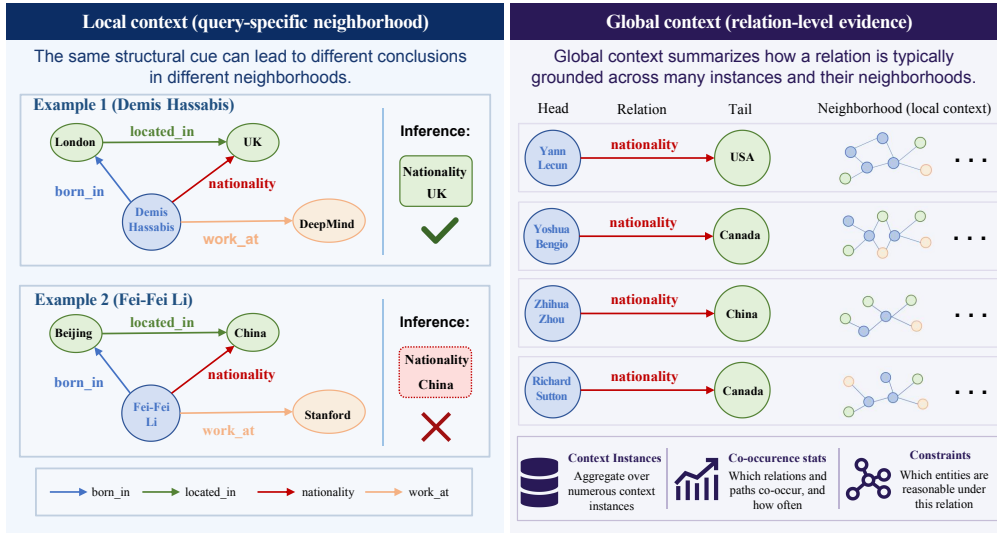


Figure 1: (a) **Left: Local context.** The same structural cue may support different conclusions depending on the query-specific neighborhood. (b) **Right: Global context.** Global context summarizes how a relation is typically instantiated across many examples, together with their associated neighborhoods.

combines feature-level attention with sample-level attention. Through multi-graph pre-training on diverse knowledge graphs, KGPFN learns to jointly exploit structural invariances and contextual cues, enabling zero-shot transfer and in-context adaptation to previously unseen graphs. The main contributions of this work include: The main contributions of this work are summarized as follows:

- **Local and global context construction for KGs.** We introduce a context construction strategy tailored to knowledge graph foundation models. Unlike existing KG foundation models that mainly emphasize transferable relational patterns, our approach explicitly builds both local and global context: local context characterizes the query-specific neighborhood, while global context captures relation-level regularities across many instances of the query relation.
- **In-context learning over KG context via Prior-data Fitted Networks.** We propose KGPFN, which leverages the Prior-data Fitted Network paradigm to perform in-context learning over structured KG context. Through feature-level attention and sample-level attention, KGPFN learns to exploit both intra-instance structural signals and inter-instance relational regularities, enabling inference-time adaptation to unseen graphs without fine-tuning.
- **State-of-the-art results with in-context learning alone.** Extensive experiments on diverse KG benchmarks show that KGPFN achieves state-of-the-art performance in both inductive and full-inductive settings. Remarkably, KGPFN outperforms competitive fine-tuned KG foundation model baselines using only in-context learning, demonstrating the power of context-based adaptation for knowledge graph reasoning.

2 Related Work

Knowledge graph foundation models. Current KGFM models largely aim to capture relation invariants that transfer across heterogeneous KGs, enabling fully-inductive, zero-shot completion on unseen entities and relations. ULTRA [16] instantiates this idea by building a relation graph from four fundamental interaction patterns and learning transferable, query-conditioned relation representations. TRIX [48] further strengthens expressiveness by encoding which-entity participation in relation interactions and iteratively co-updating entity and relation embeddings, supporting efficient relation prediction. From a unifying viewpoint, MOTIF [23] shows that many KGFM models rely on binary motifs, and that lifting to higher-order motifs via relational hypergraphs yields provably stronger expressiveness.

In parallel, KG-ICL [12] frames KG reasoning as in-context learning, using a few query-centered prompt graphs (e.g., 5-shot) plus a unified tokenizer to align entities/reactions across KGs for universal generalization.

In-context learning for structured data via Prior-data Fitted Networks. Prior-data Fitted Networks (PFNs) [31] formulate in-context learning as Bayesian inference over structured datasets. A PFN is pretrained on synthetic tasks sampled from a prior, and learns to predict query labels from a set of labeled context examples in a single forward pass, without task-specific optimization. TabPFN [22] instantiates this idea for tabular data by treating table rows as context examples, achieving strong small-data performance; recent variants such as TabPFN-v2.5 [19], TabICL [33], and Limix [47] further improve robustness and scalability to larger tables. More broadly, PFN-based models have begun to extend beyond tabular task to other structure data, including time-series [41], relational database [45] and graph tasks [14, 27].

3 Preliminary

3.1 Task Definition

Notation. A knowledge graph (KG) is a directed multi-relational graph $\mathcal{G} = (\mathcal{E}, \mathcal{R}, \mathcal{T})$, where \mathcal{E} denote the entity set, \mathcal{R} denote the relation set, and $\mathcal{T} \subseteq \mathcal{E} \times \mathcal{R} \times \mathcal{E}$ denote the observed triple set respectively. Each triple $(h, r, t) \in \mathcal{T}$ represents a directed edge from the head entity h to the tail entity t under relation r .

Problem Definition. In this paper, we study the link prediction task: given an incomplete query $(h, r, ?)$, predict the missing tail entity t from candidate entities. Formally, a model assigns a plausibility score $s(h, r, t)$ to each candidate $t \in \mathcal{E}$ and ranks candidates accordingly. We consider two evaluation settings. In the *transductive* setting, the entity set is fixed across training and test; the model is trained on $\mathcal{T}_{\text{train}}$ and evaluated on held-out triples $\mathcal{T}_{\text{test}}$, where all entities appearing in $\mathcal{T}_{\text{test}}$ also appear in $\mathcal{T}_{\text{train}}$, allowing the model to learn entity-specific representations. In the *inductive* setting, the test graph $\mathcal{G}_{\text{test}} = (\mathcal{E}_{\text{test}}, \mathcal{R}, \mathcal{T}_{\text{test}})$ contains entities unseen during training, i.e., $\mathcal{E}_{\text{test}} \cap \mathcal{E}_{\text{train}} = \emptyset$; the model must generalize to these new entities based on relational structure without any parameter updates.

3.2 Prior-data Fitted Networks

Posterior predictive distribution. In the Bayesian view of supervised learning, a prior specifies a hypothesis space Φ that maps inputs x to labels y . Each hypothesis $\phi \in \Phi$ induces a data-generating distribution, from which a dataset $D = \{(x_i, y_i)\}_{i=1}^n$ can be sampled. Given a context (training) set D and a test input x , the posterior predictive distribution (PPD) marginalizes over hypotheses:

$$p(y | x, D) \propto \int_{\Phi} p(y | x, \phi) p(D | \phi) p(\phi) d\phi, \quad (1)$$

where $p(\phi)$ is the prior weight of hypothesis ϕ and $p(D | \phi)$ is the likelihood of observing D under ϕ .

Prior-data fitted networks for structured-data foundation models. Prior-data fitted networks (PFNs) cast in-context learning as amortized Bayesian inference: a single parametric model is trained to output the posterior predictive distribution conditioned on a set of labeled context examples. Concretely, given a labeled support set $\mathcal{C} = \{(x_c^{(i)}, y_c^{(i)})\}_{i=1}^n$ and a query input x_q , a PFN produces a predictive distribution over the query label:

$$f_{\theta}(x_q, \mathcal{C}) \approx p(y_q | x_q, \mathcal{C}), \quad (2)$$

At inference time, a PFN approximates Bayesian-style posterior prediction by treating the context set \mathcal{C} as observed evidence and conditioning on it to produce a predictive distribution for the query. In this view, the pretrained network encodes an implicit prior over tasks, while the observed context induces an approximate posterior predictive distribution, which achieved purely through feed-forward computation without any parameter updates.

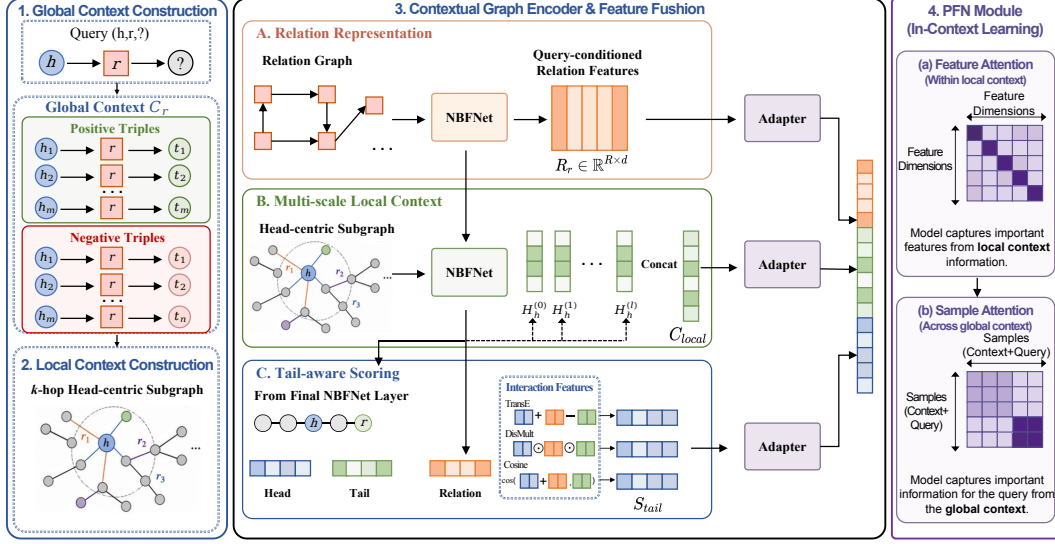


Figure 2: The framework of KGPFN.

4 Method

In this section, we introduce our KGPFN, a knowledge graph foundational model with in-context learning capabilities. The framework of KGPFN is shown in Fig. 2. In Section 4.1 and 4.2, we introduced how to construct global and local contexts respectively. In Section 4.3, we presented how to encode the obtained contexts. In Section 4.4, we introduced the PFN architecture used, which consists of feature attention and sample attention.

4.1 Global Context Construction

To expose the model to typical grounding patterns of a specific relation, we first construct a relation-specific global context. For a given query $(h, r, ?)$, we collect a set of observed triples of the same relation from the graph, $\{(h_i, r, t_i)\}_{i=1}^{m^+}$, so that the context reflects how r is realized in the data. To additionally indicate when a candidate completion should not hold, we generate a set of negative triples for the same relation, $\{(h_j, r, t_j)\}_{j=1}^{m^-}$, via negative sampling. We merge them into a single global context set $\mathcal{C}_r = \{((h_k, r, t_k), y_k)\}_{k=1}^m$, where $m = m^+ + m^-$ and $y_k \in \{0, 1\}$ is the binary label with $y_k = 1$ for positives and $y_k = 0$ for negatives. This global context provides macroscopic relational patterns for the task.

4.2 Local Context Construction

While the global context provides relation-level priors, local structural information is crucial for disambiguating specific entities. For each individual triple (including the query and the global context triples), we extract its local context. A straightforward way to construct local context for a candidate triple (h, r, t) is to build an enclosing subgraph around both h and t . However, jointly extracting $\mathcal{N}_k(h) \cup \mathcal{N}_k(t)$ for every candidate t is prohibitively expensive for large-scale training and inference. To enable efficient batching and fast querying, we instead construct local context only from the head entity by extracting a k -hop neighborhood around h . That is to say, given a triple with head h , we define the head-centric k -hop neighborhood as $\mathcal{V}_h^{(k)} = \mathcal{N}_k(h)$ and $\mathcal{G}_h^{(k)} = \mathcal{G}[\mathcal{V}_h^{(k)}]$, where $\mathcal{N}_k(\cdot)$ denotes the set of nodes within k hops. This construction is independent of the candidate tail t , and thus scales naturally to large candidate sets.

4.3 Contextual Graph Encoder

With the global and local contexts constructed, we employ a unified encoder to map these symbolic structures into continuous vector spaces.

Relation representations. Following previous methods [16, 48], we first build the relation graph $\mathcal{G}_r = (\mathcal{R}, \mathcal{R}_{\text{fund}}, \mathcal{E}_r)$ from the original KG, where each node corresponds to a relation type in \mathcal{R} . Edges in \mathcal{E}_r encode how two relations interact through shared endpoints. We consider four fundamental interaction types $\mathcal{R}_{\text{fund}} = \{\text{t2h}, \text{h2h}, \text{h2t}, \text{t2t}\}$. Equivalently, the relation graph can be represented by an adjacency tensor $\mathbf{A}_r \in \mathbb{R}^{|\mathcal{R}| \times |\mathcal{R}| \times 4}$.

Given a query relation r , we compute conditional relation representations by initializing the query-relation node in the relation graph \mathcal{G}_r with an indicator label (set $\mathbf{h}_{r|r}^{(0)} = \mathbf{1}^d$ and $\mathbf{h}_{v|r}^{(0)} = \mathbf{0}$ for all $v \neq r$), and then running message passing on \mathcal{G}_r . Each layer aggregates messages from neighbors connected by the four fundamental interaction types $s \in \mathcal{R}_{\text{fund}}$:

$$\mathbf{h}_{v|r}^{(\ell+1)} = \text{Upd}\left(\mathbf{h}_{v|r}^{(\ell)}, \text{Agg}\left(\{\text{Msg}_s(\mathbf{h}_{u|r}^{(\ell)}) : u \in \mathcal{N}_s(v), s \in \mathcal{R}_{\text{fund}}\}\right)\right), \quad (3)$$

where ℓ indexes the message-passing layer. After L_r layers, we obtain a matrix of query-conditioned relation embeddings $\mathbf{R}_r = [\mathbf{h}_{v|r}^{(L_r)}]_{v \in \mathcal{R}} \in \mathbb{R}^{|\mathcal{R}| \times d}$.

Multi-scale local context representation. Then, we encode the head-centric neighborhood $\mathcal{G}_h^{(k)}$ using an L -layer NBFNet, conditioned on the query relation embedding \mathbf{r} . Let $\mathbf{H}_v^{(\ell)}$ be the node representation at layer ℓ . Each layer propagates relation-aware messages along typed edges:

$$\mathbf{H}_v^{(\ell+1)} = \text{Upd}\left(\mathbf{H}_v^{(\ell)}, \text{Agg}\left(\{\text{Msg}(\mathbf{H}_u^{(\ell)}, r_{u \rightarrow v}, \mathbf{r}) : (u, r_{u \rightarrow v}, v) \in \mathcal{T} \cap \mathcal{G}_h^{(k)}\}\right)\right). \quad (4)$$

An important property of NBFNet is that the representation after ℓ layers aggregates evidence from up to ℓ hops. Therefore, we directly treat the head node embedding at each layer as a subgraph summary vector. Formally, we set $\mathbf{c}_{\text{loc}}^{(\ell)}(h, r) = \mathbf{H}_h^{(\ell)}$, and form the multi-scale local-context sequence $\mathbf{C}_{\text{loc}}(h, r) = [\mathbf{c}_{\text{loc}}^{(1)}; \dots; \mathbf{c}_{\text{loc}}^{(L)}]$.

Tail-aware scoring representation. To distinguish different tail entities efficiently, we additionally retrieve the tail embedding at the last NBFNet layer, denoted as $\mathbf{z}_t^{(L)}$, and apply a lightweight structure feature enhancement on top of it to better encode its structural signal within the k -hop neighborhood. We then combine the query-specific head representation $\mathbf{z}_h^{(L)}$, the query relation embedding \mathbf{r} , and the tail representation $\mathbf{z}_t^{(L)}$ to form interaction features:

$$\phi_{\text{trans}}(h, r, t) = \mathbf{z}_h^{(L)} + \mathbf{r} - \mathbf{z}_t^{(L)}, \phi_{\text{distmult}}(h, r, t) = \mathbf{z}_h^{(L)} \odot \mathbf{r} \odot \mathbf{z}_t^{(L)}, \phi_{\text{cos}}(h, r, t) = \cos(\mathbf{z}_h^{(L)} + \mathbf{r}, \mathbf{z}_t^{(L)}) \quad (5)$$

We then obtain the tail-aware score representation by combining the above three interaction features: $S_{\text{tail}}(h, r, t) = [\phi_{\text{trans}}(h, r, t), \phi_{\text{distmult}}(h, r, t), \phi_{\text{cos}}(h, r, t)]$. For each context pair $((h_k, r, t_k), y_k) \in \mathcal{C}_r$ as well as the query, we align the three heterogeneous features generated by the encoder into a shared latent space via three lightweight adapters and concatenate them to form a single fused embedding:

$$\mathbf{x}_k = \left[\text{Adapter}(\mathbf{C}_{\text{loc}}(h_k, r)) ; \text{Adapter}([\mathbf{z}_{h_k}^{(L)}; \mathbf{r}; \mathbf{z}_{t_k}^{(L)}]) ; \text{Adapter}(S_{\text{tail}}(h_k, r, t_k)) \right], \quad (6)$$

where $\text{Adapter}(\cdot)$ is a lightweight projection module implemented as an MLP followed by normalization.

4.4 PFN Architecture

After fusing the representations in Eq. (6), we estimate the plausibility score $s(h, r, t)$ by feeding the query representation \mathbf{x}_q and the relation-specific labeled context set $\mathcal{C}_r = \{(\mathbf{x}_i, y_i)\}_{i=1}^m$ into the PFN architecture defined in Eq. (2), where $y_i \in \{0, 1\}$ denotes whether the corresponding context triple is positive or negative. The PFN module consists of two key attention mechanisms: feature-level self-attention, which refines the feature dimensions of each sample, and sample-level attention,

which aggregates evidence across context examples. Specifically, we first apply self-attention over \mathcal{C}_r to capture dependencies among context samples. We then use cross-attention from the query representation \mathbf{x}_q to the context set \mathcal{C}_r , allowing the query to retrieve relation-specific evidence from the labeled context. RoPE [39] is incorporated into the attention blocks as positional encoding. Finally, the query-conditioned contextual evidence is combined with \mathbf{x}_q to produce the plausibility score $s(h, r, t)$.

Training Objective. We train KGPFN with two complementary objectives under negative sampling. First, we use a binary cross-entropy (BCE) loss to directly separate positives from negatives and encourage discriminative plausibility scores:

$$\mathcal{L}_{\text{BCE}} = -\frac{1}{B} \sum_{i=1}^B \left[\log \sigma(s_i^+) + \sum_{j=1}^N w_{i,j} \log(1 - \sigma(s_{i,j}^-)) \right], \quad (7)$$

where $\sigma(\cdot)$ is the sigmoid function and $w_{i,j} = \frac{\exp(s_{i,j}^-/\tau)}{\sum_{k=1}^N \exp(s_{i,k}^-/\tau)}$ is a hard adaptive weight for the j -th negative with temperature τ . Second, we additionally adopt a softmax cross-entropy loss to explicitly enforce that the positive triple is ranked above its sampled negatives:

$$\mathcal{L}_{\text{CE}} = -\frac{1}{B} \sum_{i=1}^B \log \frac{\exp(s_i^+)}{\exp(s_i^+) + \sum_{j=1}^N \exp(s_{i,j}^-)}. \quad (8)$$

Finally, the overall training objective is the sum of them $\mathcal{L} = \mathcal{L}_{\text{BCE}} + \mathcal{L}_{\text{CE}}$.

4.5 Theoretical Insight

We provide a theoretical insight into how KGPFN extends relational modeling from **structural expressivity** to **functional expressivity**. Prior KG foundation models [16, 48, 23] primarily focus on learning structure-level invariants, what motifs or relational patterns are present around a triple, and thus excel at capturing transferable structural evidence. However, zero-shot reasoning on unseen relations additionally requires how such motifs should be combined into a relation-specific decision rule. KGPFN addresses this by leveraging the labeled global context to infer the functional relevance of local structural patterns and compose them into an adaptive scoring function.

Theorem 1 (Functional Expressivity via In-context Composition). *Let q be a query triple and \mathcal{S}_r be the in-context support set of triple pairs for a relation r . Let $c_{M_k}(\cdot)$ denote the structural count of the k -th topological structural pattern/motif M_k extracted by the encoder. Assume the PFN attention projection matrices satisfy $\mathbf{W}_Q^\top \mathbf{W}_K = \mathbf{I}$, and the encoder’s latent motif basis is orthogonal such that $\mathbf{W}_M^\top \mathbf{W}_M = \mathbf{\Lambda} = \text{diag}(\lambda_1, \dots, \lambda_n)$. Under a linear attention regime, the PFN instantiates a context-conditioned scoring function, where relation-specific evidence is composed on the fly from the query and the in-context support set:*

$$P(q \in r \mid \mathcal{S}_r) \propto \sum_{k=1}^n \lambda_k \cdot c_{M_k}(q) \cdot \mathbb{E}_{s \sim \mathcal{S}_r} [c_{M_k}(s)] \quad (9)$$

where the term $c_{M_k}(q) \mathbb{E}_{s \sim \mathcal{S}_r} [c_{M_k}(s)]$ can be interpreted as a soft conjunction: a structural pattern contributes strongly only when it is present in the query and salient in the in-context support set.

Theorem 1 shows that KGPFN scores a query by aligning its local structural evidence with label-weighted pattern statistics inferred from the in-context support set. Consequently, structural patterns are not assigned fixed, relation-specific weights; rather, their functional relevance is estimated on the fly from context, enabling adaptation to unseen relations without parameter updates.

5 Experiments

5.1 Experimental Setup

Datasets and Metrics. Following [16, 48], we evaluate on 57 knowledge graphs from diverse domains under three settings: *Transductive* (16 datasets), where all test-time entities and relations are

Table 1: Average MRR and Hits@10 over 57 KGs. (**Bold**: best; Underline: runner-up.)

Setting	Model	Inductive e, r (23 graphs)		Inductive e (18 graphs)		Transductive (16 graphs)		Total Avg (57 graphs)		Pretraining (3 graphs)	
		MRR	H@10	MRR	H@10	MRR	H@10	MRR	H@10	MRR	H@10
Zero-shot	ULTRA	0.345	0.513	0.431	0.566	0.329	0.479	0.367	0.520	–	–
	KGICL	0.362	0.544	0.440	0.584	0.346	0.493	0.382	0.542	–	–
	Motif	0.337	0.509	0.431	0.570	0.335	0.492	0.370	0.527	–	–
	TRIX	0.368	0.540	0.455	0.592	0.342	0.522	0.388	0.551	–	–
Fine-tuned	ULTRA	0.397	0.556	0.442	0.582	0.384	0.548	0.407	0.562	0.407	0.568
	KGICL	<u>0.426</u>	<u>0.616</u>	<u>0.464</u>	<u>0.630</u>	0.397	0.554	<u>0.430</u>	<u>0.603</u>	–	–
	Motif	0.401	0.558	0.455	0.594	0.390	0.549	0.415	0.569	0.415	0.565
	TRIX	0.401	0.556	0.459	0.594	0.390	<u>0.558</u>	0.418	0.569	0.415	0.563
In-context	KGPFN	0.433	0.639	0.465	0.638	<u>0.393</u>	0.600	0.432	0.628	0.423	0.623

seen during training; *Inductive* (18 datasets), where test-time entities are unseen but relations are seen during training; and *Fully Inductive* (23 datasets), where both entities and relations are unseen at test time. We adopt filtered ranking metrics. For each test triple (h, r, t) , we rank the tail entity against all candidates, filtering out other valid triples. We report the average Mean Reciprocal Rank (MRR) and Hits@10 after 5 runs. For more details about the datasets, please see Appendix B.1.

Baselines. We compare KGPFN with several advanced KG foundation models, including **ULTRA** [16], a universal pretraining framework for transferable inductive KG reasoning across diverse graphs and relation vocabularies; **KG-ICL** [12], a prompt-based KG foundation model that performs KG reasoning via in-context learning over retrieved triples; **TRIX** [48], an expressive fully-inductive model designed for zero-shot domain transfer in KG completion; and **MOTIF** [23], a motif-based KG foundation model that captures higher-order relational interaction patterns beyond pairwise relation compositions.

Implementation Details. For the contextual graph encoder, we follow the design of [16]: the relation encoder and the local-context encoder each use a 6-layer NBFNet with hidden dimension 64. For the PFN transformer, we adopt the pretrained TabICL [34] architecture and remove its feature preprocessing module. For local context, we extract the query-centered 3-hop enclosing subgraph around the head entities. For global context, we include 20 positive triples and 60 negative triples. We optimize the model with AdamW using a learning rate of 5×10^{-4} and weight decay 10^{-6} . During training, we sample 64 negatives per positive query triple; during evaluation, we rank against all entities. We use adversarial negative sampling with temperature $\tau = 1.0$ to weight hard negatives. All experiments are run on 8 NVIDIA A800 80GB GPUs.

5.2 In-context Inference

Following prior KG foundation model setups [16, 48, 23], we pretrain KGPFN on three graphs: FB15K-237 [43], WN18RR [13], and CodexMedium [37], and compare it with several state-of-the-art KG foundation models. Since KG-ICL is pretrained on a different set of graphs, we do not report its results on datasets overlapping with these three pretraining graphs. Finally, as KGPFN retrieves relation-relevant positive and negative instances from the target graph as context at inference time, no additional finetuning is performed; all results are obtained by directly applying in-context inference after pretraining.

The results have been reported in Table 1. Overall, KGPFN achieves the best average performance across 57 knowledge graphs. It obtains state-of-the-art Hits@10 under all three evaluation settings, and reaches state-of-the-art MRR in the two inductive settings. Notably, in the full-inductive regime, the most challenging setting, KGPFN’s advantage becomes even more pronounced. As the task becomes harder, from transductive to inductive and full-inductive settings, the performance gap between KGPFN and competing models consistently widens. These results suggest that our model can effectively leverage in-context reasoning, outperforming competing methods even when they are finetuned on each target dataset. Detailed results of our model and additional results with alternative PFN architectures [47] are provided in Appendix B.2.

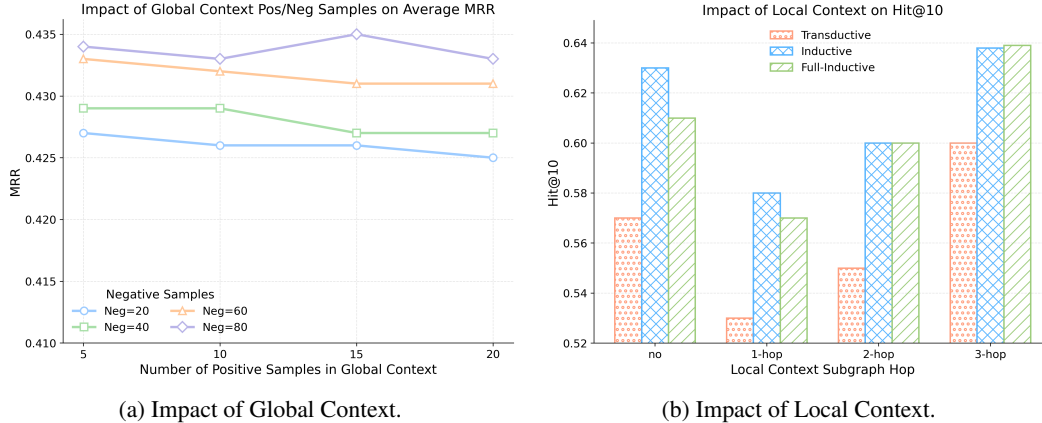


Figure 3: Global and Local Context Sensitivity Analysis.

5.3 Context Sensitivity Analysis

We further analyzed the impact of different numbers of contexts on the model’s performance.

Global Context. We evaluate a range of global-context configurations. Specifically, we vary the number of positive instances (5, 10, 15, and 20) and the number of negative instances (20, 40, 60, and 80), and consider all pairwise combinations. We report the average MRR across 23 full-inductive tasks, as shown in the Fig 3a. Overall, changing the number of positive instances has no noticeable effect on performance, indicating that KGPFN is robust to the amount of positive context. In contrast, increasing the number of negative instances consistently improves performance. This suggests that the model already distinguishes positive instances well; however, for ranking-based metrics such as MRR, separating hard negative candidates is often more critical. Consequently, providing more negative instances in the global context yields more reliable rankings and better overall results.

Local Context. We evaluate the effect of local context by varying the maximum neighborhood radius for extracting subgraph vectors from 0 to 3 hops. As shown in Fig. 3b, we observe a trend consistent with the context analysis in KGICL [12]: using only 1-hop or 2-hop neighborhoods leads to varying degrees of performance degradation. This suggests that shallow local context may provide insufficient support for effective reasoning. Intuitively, for many target relations, one- or two-hop information is often inadequate to capture compositional evidence formed by multiple relations, which typically requires multi-hop neighborhoods.

5.4 Visualization

To intuitively illustrate how the model selects informative positive and negative instances from the global context, we present a case study on CodexLarge [37] with the query (Imperial, -Record label, ?). We construct a candidate set with 5 ground-truth tails and 20 incorrect tails, and sample a global context containing 5 positive and 20 negative instances. We visualize the cross-attention weights from the last layer of the sample-attention module, showing how each query candidate attends to the context instances. As shown in Fig. 4, correct tail candidates place highly concentrated attention on positive context instances, whereas incorrect candidates show more dispersed attention over negative context instances. These results suggest that KGPFN effectively exploits global context during inference to guide and sharpen query predictions.

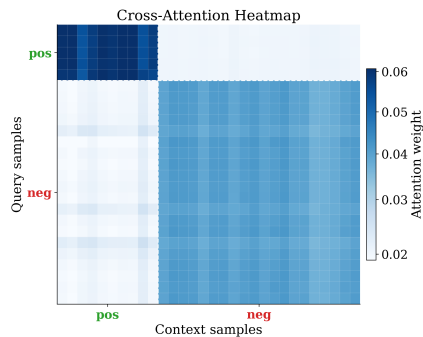


Figure 4: The heatmap of sample attention.

6 Conclusion

We study in-context learning for knowledge graph foundation models and argue that effective in-context reasoning requires both query-specific local context and relation-level global context. To this end, we propose KGPFN, which combines a local context encoder with a PFN-based global-context aggregator to produce relation-adaptive predictions at inference time. Extensive experiments show state-of-the-art performance in both inductive and full-inductive settings, demonstrating the benefits of unifying global and local context for KG in-context adaptation.

References

- [1] Rishabh Agarwal, Avi Singh, Lei Zhang, Bernd Bohnet, Luis Rosias, Stephanie Chan, Biao Zhang, Ankesh Anand, Zaheer Abbas, Azade Nova, et al. Many-shot in-context learning. *Advances in Neural Information Processing Systems*, 37:76930–76966, 2024.
- [2] Jiaxin Bai, Xin Liu, Weiqi Wang, Chen Luo, and Yangqiu Song. Complex query answering on eventuality knowledge graph with implicit logical constraints. *Advances in Neural Information Processing Systems*, 36:30534–30553, 2023.
- [3] Jiaxin Bai, Zihao Wang, Hongming Zhang, and Yangqiu Song. Query2particles: Knowledge graph reasoning with particle embeddings. In *Findings of the Association for Computational Linguistics: NAACL 2022*, pages 2703–2714, 2022.
- [4] Jiaxin Bai, Zihao Wang, Yukun Zhou, Hang Yin, Weizhi Fei, Qi Hu, Zheyang Deng, Jiayang Cheng, Tianshi Zheng, Hong Ting Tsang, et al. Top ten challenges towards agentic neural graph databases. *arXiv preprint arXiv:2501.14224*, 2025.
- [5] Pablo Barceló, Egor V Kostylev, Mikael Monet, Jorge Pérez, Juan Reutter, and Juan Pablo Silva. The logical expressiveness of graph neural networks. In *International conference on learning representations*, 2020.
- [6] Maciej Besta, Patrick Iff, Florian Scheidl, Kazuki Osawa, Nikoli Dryden, Michal Podstawski, Tiancheng Chen, and Torsten Hoefer. Neural graph databases. In *Learning on Graphs Conference*, pages 31–1. PMLR, 2022.
- [7] Antoine Bordes, Nicolas Usunier, Alberto Garcia-Duran, Jason Weston, and Oksana Yakhnenko. Translating embeddings for modeling multi-relational data. *Advances in neural information processing systems*, 26, 2013.
- [8] Yixin Cao, Xiang Wang, Xiangnan He, Zikun Hu, and Tat-Seng Chua. Unifying knowledge graph learning and recommendation: Towards a better understanding of user preferences. In *The world wide web conference*, pages 151–161, 2019.
- [9] Mingyang Chen, Wen Zhang, Wei Zhang, Qiang Chen, and Huajun Chen. Meta relational learning for few-shot link prediction in knowledge graphs. In *Proceedings of the 2019 conference on empirical methods in natural language processing and the 9th international joint conference on natural language processing (EMNLP-IJCNLP)*, pages 4217–4226, 2019.
- [10] Zhengdao Chen, Lei Chen, Soledad Villar, and Joan Bruna. Can graph neural networks count substructures? *Advances in neural information processing systems*, 33:10383–10395, 2020.
- [11] Tsz Ting Chung, Lemao Liu, Mo Yu, and Dit-Yan Yeung. Many-shot cot-icl: Making in-context learning truly learn, 2026.
- [12] Yuanning Cui, Zequn Sun, and Wei Hu. A prompt-based knowledge graph foundation model for universal in-context reasoning. *Advances in Neural Information Processing Systems*, 37:7095–7124, 2024.
- [13] Tim Dettmers, Pasquale Minervini, Pontus Stenetorp, and Sebastian Riedel. Convolutional 2d knowledge graph embeddings. In *Proceedings of the AAAI conference on artificial intelligence*, volume 32, 2018.

- [14] Dmitry Ereemeev, Oleg Platonov, Gleb Bazhenov, Artem Babenko, and Liudmila Prokhorenkova. Graphpfn: A prior-data fitted graph foundation model. *arXiv preprint arXiv:2509.21489*, 2025.
- [15] Mikhail Galkin, Max Berrendorf, and Charles Tapley Hoyt. An open challenge for inductive link prediction on knowledge graphs. *arXiv preprint arXiv:2203.01520*, 2022.
- [16] Mikhail Galkin, Xinyu Yuan, Hesham Mostafa, Jian Tang, and Zhaocheng Zhu. Towards foundation models for knowledge graph reasoning. *arXiv preprint arXiv:2310.04562*, 2023.
- [17] Yisen Gao, Jiaxin Bai, Yi Huang, Xingcheng Fu, Qingyun Sun, and Yangqiu Song. Unifying deductive and abductive reasoning in knowledge graphs with masked diffusion model. In *Proceedings of the ACM Web Conference 2026*, pages 3600–3611, 2026.
- [18] Yisen Gao, Jiaxin Bai, Tianshi Zheng, Qingyun Sun, Ziwei Zhang, Xingcheng Fu, Jianxin Li, and Yangqiu Song. Controllable logical hypothesis generation for abductive reasoning in knowledge graphs. *arXiv preprint arXiv:2505.20948*, 2025.
- [19] Léo Grinsztajn, Klemens Flöge, Oscar Key, Felix Birkel, Philipp Jund, Brendan Roof, Benjamin Jäger, Dominik Safaric, Simone Alessi, Adrian Hayler, et al. Tabpfn-2.5: Advancing the state of the art in tabular foundation models. *arXiv preprint arXiv:2511.08667*, 2025.
- [20] Takuo Hamaguchi, Hidekazu Oiwa, Masashi Shimbo, and Yuji Matsumoto. Knowledge transfer for out-of-knowledge-base entities: A graph neural network approach. *arXiv preprint arXiv:1706.05674*, 2017.
- [21] Daniel Scott Himmelstein, Antoine Lizee, Christine Hessler, Leo Brueggeman, Sabrina L Chen, Dexter Hadley, Ari Green, Pouya Khankhanian, and Sergio E Baranzini. Systematic integration of biomedical knowledge prioritizes drugs for repurposing. *elife*, 6:e26726, 2017.
- [22] Noah Hollmann, Samuel Müller, Katharina Eggenberger, and Frank Hutter. Tabpfn: A transformer that solves small tabular classification problems in a second. *arXiv preprint arXiv:2207.01848*, 2022.
- [23] Xingyue Huang, Pablo Barceló, Michael M Bronstein, Ismail Ilkan Ceylan, Mikhail Galkin, Juan L Reutter, and Miguel Romero Orth. How expressive are knowledge graph foundation models? *arXiv preprint arXiv:2502.13339*, 2025.
- [24] Jaejun Lee, Chanyoung Chung, and Joyce Jiyoung Whang. Ingram: Inductive knowledge graph embedding via relation graphs. In *International conference on machine learning*, pages 18796–18809. PMLR, 2023.
- [25] Jens Lehmann, Robert Isele, Max Jakob, Anja Jentzsch, Dimitris Kontokostas, Pablo N Mendes, Sebastian Hellmann, Mohamed Morsey, Patrick Van Kleef, Sören Auer, et al. Dbpedia—a large-scale, multilingual knowledge base extracted from wikipedia. *Semantic web*, 6(2):167–195, 2015.
- [26] Yufei Li, Yisen Gao, Jiaxin Bai, Jiaxuan Xiong, Haoyu Huang, Zhongwei Xie, Hong Ting Tsang, and Yangqiu Song. Towards neural graph data management. *arXiv preprint arXiv:2603.05529*, 2026.
- [27] Tianyin Liao, Chunyu Hu, Yicheng Sui, Xingxuan Zhang, Peng Cui, Jianxin Li, and Ziwei Zhang. Tfmlinker: Universal link predictor by graph in-context learning with tabular foundation models. *arXiv preprint arXiv:2602.08592*, 2026.
- [28] Aixin Liu, Bei Feng, Bing Xue, Bingxuan Wang, Bochao Wu, Chengda Lu, Chenggang Zhao, Chengqi Deng, Chenyu Zhang, Chong Ruan, et al. Deepseek-v3 technical report. *arXiv preprint arXiv:2412.19437*, 2024.
- [29] Shuwen Liu, Bernardo Grau, Ian Horrocks, and Egor Kostylev. Indigo: Gnn-based inductive knowledge graph completion using pair-wise encoding. *Advances in Neural Information Processing Systems*, 34:2034–2045, 2021.
- [30] Tom Mitchell, William Cohen, Estevam Hruschka, Partha Talukdar, Bishan Yang, Justin Betteridge, Andrew Carlson, Bhavana Dalvi, Matt Gardner, Bryan Kisiel, et al. Never-ending learning. *Communications of the ACM*, 61(5):103–115, 2018.

- [31] Thomas Nagler. Statistical foundations of prior-data fitted networks. In *International Conference on Machine Learning*, pages 25660–25676. PMLR, 2023.
- [32] OpenAI. GPT-4 technical report. *CoRR*, abs/2303.08774, 2023.
- [33] Jingang Qu, David Holzmüller, Gaël Varoquaux, and Marine Le Morvan. Tabicl: A tabular foundation model for in-context learning on large data. *arXiv preprint arXiv:2502.05564*, 2025.
- [34] Jingang Qu, David Holzmüller, Gaël Varoquaux, and Marine Le Morvan. Tabiclv2: A better, faster, scalable, and open tabular foundation model. *arXiv preprint arXiv:2602.11139*, 2026.
- [35] Hongyu Ren, Mikhail Galkin, Michael Cochez, Zhaocheng Zhu, and Jure Leskovec. Neural graph reasoning: Complex logical query answering meets graph databases. *arXiv preprint arXiv:2303.14617*, 2023.
- [36] Hongyu Ren, Weihua Hu, and Jure Leskovec. Query2box: Reasoning over knowledge graphs in vector space using box embeddings. *arXiv preprint arXiv:2002.05969*, 2020.
- [37] Tara Safavi and Danai Koutra. Codex: A comprehensive knowledge graph completion benchmark. In *Proceedings of the 2020 Conference on Empirical Methods in Natural Language Processing (EMNLP)*, pages 8328–8350, 2020.
- [38] Robyn Speer, Joshua Chin, and Catherine Havasi. Conceptnet 5.5: An open multilingual graph of general knowledge. In *Proceedings of the AAAI conference on artificial intelligence*, volume 31, 2017.
- [39] Jianlin Su, Murtadha Ahmed, Yu Lu, Shengfeng Pan, Wen Bo, and Yunfeng Liu. Roformer: Enhanced transformer with rotary position embedding. *Neurocomputing*, 568:127063, 2024.
- [40] Fabian M Suchanek, Gjergji Kasneci, and Gerhard Weikum. Yago: a core of semantic knowledge. In *Proceedings of the 16th international conference on World Wide Web*, pages 697–706, 2007.
- [41] Ege Onur Taga, Muhammed Emrullah Ildiz, and Samet Oymak. Timepfn: Effective multivariate time series forecasting with synthetic data. In *Proceedings of the AAAI conference on artificial intelligence*, volume 39, pages 20761–20769, 2025.
- [42] Komal Teru, Etienne Denis, and Will Hamilton. Inductive relation prediction by subgraph reasoning. In *International conference on machine learning*, pages 9448–9457. PMLR, 2020.
- [43] Kristina Toutanova and Danqi Chen. Observed versus latent features for knowledge base and text inference. In *Proceedings of the 3rd workshop on continuous vector space models and their compositionality*, pages 57–66, 2015.
- [44] Hugo Touvron, Thibaut Lavril, Gautier Izacard, Xavier Martinet, Marie-Anne Lachaux, Timothée Lacroix, Baptiste Rozière, Naman Goyal, Eric Hambro, Faisal Azhar, et al. Llama: Open and efficient foundation language models. *arXiv preprint arXiv:2302.13971*, 2023.
- [45] Yanbo Wang, Jiaxuan You, Chuan Shi, and Muhan Zhang. Relational in-context learning via synthetic pre-training with structural prior. *arXiv preprint arXiv:2603.03805*, 2026.
- [46] Zhongwei Xie, Jiaxin Bai, Shujie Liu, Haoyu Huang, Yufei Li, Yisen Gao, Hong Ting Tsang, and Yangqiu Song. Ngdb-zoo: Towards efficient and scalable neural graph databases training. *arXiv preprint arXiv:2602.21597*, 2026.
- [47] Xingxuan Zhang, Gang Ren, Han Yu, Hao Yuan, Hui Wang, Jiansheng Li, Jiayun Wu, Lang Mo, Li Mao, Mingchao Hao, et al. Limix: Unleashing structured-data modeling capability for generalist intelligence. *arXiv preprint arXiv:2509.03505*, 2025.
- [48] Yucheng Zhang, Beatrice Bevilacqua, Mikhail Galkin, and Bruno Ribeiro. Trix: A more expressive model for zero-shot domain transfer in knowledge graphs. *arXiv preprint arXiv:2502.19512*, 2025.
- [49] Jincheng Zhou, Beatrice Bevilacqua, and Bruno Ribeiro. An ood multi-task perspective for link prediction with new relation types and nodes. *arXiv preprint arXiv:2307.06046*, 23, 2023.

A Detailed Theoretical Proofs

In this appendix, we provide the rigorous mathematical foundations for the reasoning mechanism of KGPFN. We formally prove how conditional message passing achieves structural expressivity (Lemma 2) and how the Prior-Data Fitted Network (PFN) operationalizes functional expressivity via in-context composition (Theorem 1).

A.1 Motif-Level Structural Expressivity

First, we analyze the structural expressiveness of the kg foundation model at the motif level. Let $\mathcal{G} = (\mathcal{V}, \mathcal{E}, \mathcal{R})$ be a knowledge graph with a set of relation-specific adjacency matrices $\{\mathbf{A}_{r'}\}_{r' \in \mathcal{R}}$. The target query triplet to predict is defined as (u, r, v) .

Lemma 2 (Relational Motif Basis Projection via Conditional MPNN). *Let $\mathbf{z}_{u,r,v} \in \mathbb{R}^d$ be the triplet representation extracted after L layers of relation-conditional message passing. Assuming the activation functions are analytic, there exists a latent relational motif basis matrix $\mathbf{W}_{\mathcal{M}} = [\mathbf{w}_1, \mathbf{w}_2, \dots, \mathbf{w}_n] \in \mathbb{R}^{d \times |\mathcal{M}|}$ such that $\mathbf{z}_{u,r,v}$ can be exactly expanded as a linear projection of the structural relational motif counts:*

$$\mathbf{z}_{u,r,v} = \mathbf{W}_{\mathcal{M}} \Phi(u, r, v) + \mathcal{O}(\epsilon) = \sum_{k=1}^n c_{M_k}(u, r, v) \cdot \mathbf{w}_k + \mathcal{O}(\epsilon) \quad (10)$$

where $\Phi(u, r, v) \in \mathbb{R}^{|\mathcal{M}|}$ is the ground-truth homomorphism count vector of relational motifs \mathcal{M} anchored at (u, v) and conditioned on query r , and ϵ is the approximation error which bounds to 0 as $d \rightarrow \infty$.

Proof. Consider the l -th layer of the Relational Message Passing Neural Network (R-MPNN):

$$\mathbf{H}^{(l)} = \sigma \left(\sum_{r' \in \mathcal{R}} \mathbf{A}_{r'} \mathbf{H}^{(l-1)} \mathbf{W}_{1,r'}^{(l)} + \mathbf{H}^{(l-1)} \mathbf{W}_2^{(l)} \right) \quad (11)$$

By the Stone-Weierstrass approximation theorem, any analytic activation function $\sigma(\cdot)$ (e.g., GeLU, Sigmoid) can be approximated by a Taylor polynomial of degree P . Let $\sigma(x) \approx \sum_{p=0}^P \alpha_p x^p$. Unrolling the message passing over L layers, the final representation matrix $\mathbf{H}^{(L)}$ can be expressed as a non-commutative matrix polynomial over the set of adjacency matrices $\{\mathbf{A}_{r'}\}$:

$$\mathbf{H}^{(L)} \approx \sum_{i=0}^{L \times P} \sum_{\rho \in \mathcal{R}^i} \left(\prod_{j=1}^i \mathbf{A}_{\rho_j} \right) \mathbf{H}^{(0)} \Theta_{\rho} \quad (12)$$

where $\rho = (\rho_1, \dots, \rho_i)$ denotes a specific sequence of relations (a relational path of length i), and Θ_{ρ} are the equivalent polynomial coefficient matrices learned by the GNN for that specific relational path.

The triplet representation $\mathbf{z}_{u,r,v}$ is extracted from the rows corresponding to u and v . Notice that the (x, y) -th entry of the matrix product $\prod_{j=1}^i \mathbf{A}_{\rho_j}$ exactly counts the number of relational walks following the relation sequence ρ between node x and node y . Because our initial feature $\mathbf{H}^{(0)}$ contains the one-hot indicators for u conditioned on r , the extraction $\mathbf{z}_{u,r,v} = \text{Readout}(\mathbf{h}_u^{(L)}, \mathbf{h}_v^{(L)})$ effectively computes a linear combination of relational walk counts originating from u and v that intersect within the L -hop neighborhood.

According to the theory of graph homomorphisms [10, 5], any relational subgraph motif count $c_{M_k}(u, r, v)$ (such as relational triangles, rectangles, or specific logical paths like $r_1 \wedge r_2 \rightarrow r$) can be expressed as a linear combination of relational walk counts on the graph. Therefore, there exists a linear transformation $\mathbf{W}_{\mathcal{M}}$ that maps the basis of relational walk counts to the basis of relational motif counts $\Phi(u, r, v)$. Thus, we have:

$$\mathbf{z}_{u,r,v} = \sum_{k=1}^n c_{M_k}(u, r, v) \cdot \mathbf{w}_k + \mathcal{O}(\epsilon) \quad (13)$$

where \mathbf{w}_k forms the columns of $\mathbf{W}_{\mathcal{M}}$, completing the proof. \square

A.2 Proof of Functional Expressivity

Building upon Lemma 2, we now analyze how the PFN synthesizes logical rules from a support set $\mathcal{S}_r = \{(h_s, r, t_s)\}_{s=1}^K$ without learning relation-specific static parameters. Here, we restate the Theorem 1 and then proof it.

Theorem 3 (Functional Expressivity via In-context Composition). *Let q be a query triple and \mathcal{S}_r be the in-context support set of triple pairs for a relation r . Let $c_{M_k}(\cdot)$ denote the structural count of the k -th topological structural pattern/motif M_k extracted by the encoder. Assume the PFN attention projection matrices satisfy $\mathbf{W}_Q^\top \mathbf{W}_K = \mathbf{I}$, and the encoder’s latent motif basis is orthogonal such that $\mathbf{W}_M^\top \mathbf{W}_M = \mathbf{\Lambda} = \text{diag}(\lambda_1, \dots, \lambda_n)$. Under a linear attention regime, the PFN instantiates a context-conditioned scoring function, where relation-specific evidence is composed on the fly from the query and the in-context support set:*

$$P(q \in r \mid \mathcal{S}_r) \propto \sum_{k=1}^n \lambda_k \cdot c_{M_k}(q) \cdot \mathbb{E}_{s \sim \mathcal{S}_r} [c_{M_k}(s)] \quad (14)$$

where the term $c_{M_k}(q) \mathbb{E}_{s \sim \mathcal{S}_r} [c_{M_k}(s)]$ can be interpreted as a soft conjunction: a structural pattern contributes strongly only when it is present in the query and salient in the in-context support set.

Proof. In the PFN, the cross-attention mechanism computes the output representation \mathbf{o}_q for the query q by aggregating over the support set \mathcal{S}_r . The standard scaled dot-product attention is defined as:

$$\mathbf{o}_q = \sum_{s \in \mathcal{S}_r} \frac{\exp(\mathbf{z}_q^\top \mathbf{W}_Q^\top \mathbf{W}_K \mathbf{z}_s / \sqrt{d})}{\sum_{s' \in \mathcal{S}_r} \exp(\mathbf{z}_q^\top \mathbf{W}_Q^\top \mathbf{W}_K \mathbf{z}_{s'} / \sqrt{d})} \mathbf{W}_V \mathbf{z}_s \quad (15)$$

To analyze the fundamental reasoning logic, we adopt the linear attention approximation (e.g., using the first-order Taylor expansion $\exp(x) \approx 1 + x$, or directly employing unnormalized dot-product attention kernels), yielding the unnormalized attention score:

$$A(q, s) = \mathbf{z}_q^\top \mathbf{W}_Q^\top \mathbf{W}_K \mathbf{z}_s \quad (16)$$

Substituting $\mathbf{W}_Q^\top \mathbf{W}_K = \mathbf{I}$ and applying the motif basis projection from Lemma 2 ($\mathbf{z} \approx \mathbf{W}_M \Phi$), we obtain:

$$\begin{aligned} A(q, s) &= (\mathbf{W}_M \Phi(q))^\top (\mathbf{W}_M \Phi(s)) \\ &= \Phi(q)^\top (\mathbf{W}_M^\top \mathbf{W}_M) \Phi(s) \\ &= \Phi(q)^\top \mathbf{\Lambda} \Phi(s) \end{aligned} \quad (17)$$

Since $\mathbf{\Lambda}$ is a diagonal matrix of eigenvalues λ_k , the quadratic form expands to:

$$A(q, s) = \sum_{k=1}^n \lambda_k \cdot c_{M_k}(q) \cdot c_{M_k}(s) \quad (18)$$

The final prediction probability $P(q \in r \mid \mathcal{S}_r)$ is derived by projecting the aggregated representation \mathbf{o}_q onto a relation-agnostic binary classifier vector \mathbf{w}_{cls} . Assuming the value vectors $\mathbf{W}_V \mathbf{z}_s$ for positive support samples uniformly align with the positive classification direction, the probability is directly proportional to the sum of the attention scores over the support set:

$$\begin{aligned} P(q \in r \mid \mathcal{S}_r) &\propto \sum_{s \in \mathcal{S}_r} A(q, s) \\ &= \sum_{s \in \mathcal{S}_r} \sum_{k=1}^n \lambda_k \cdot c_{M_k}(q) \cdot c_{M_k}(s) \\ &= \sum_{k=1}^n \lambda_k \cdot c_{M_k}(q) \left(\sum_{s \in \mathcal{S}_r} c_{M_k}(s) \right) \end{aligned} \quad (19)$$

Table 2: 16 Transductive datasets used in the experiments.

Dataset	Entities	Rel	Train	Valid	Test
CoDEX Small	2034	42	32888	1827	1828
CoDEX Medium	17050	51	185584	10310	10311
CoDEX Large	77951	69	551193	30622	30622
WDSinger	10282	135	16142	2163	2203
FB15k237_10	11512	237	27211	15624	18150
FB15k237_20	13166	237	54423	16963	19776
FB15k237_50	14149	237	136057	17449	20324
FB15k237	14541	237	272115	17535	20466
NELL23k	22925	200	25445	4961	4952
WN18RR	40943	11	86835	3034	3134
AristoV4	44949	1605	242567	20000	20000
Hetionet	45158	24	2025177	112510	112510
NELL995	74536	200	149678	543	2818
ConceptNet100k	78334	34	100000	1200	1200
DBpedia100k	99604	470	597572	50000	50000
YAGO310	123182	37	1079040	5000	5000

Multiplying and dividing by the support set size $K = |\mathcal{S}_r|$, we introduce the empirical expectation $\mathbb{E}_{s \sim \mathcal{S}_r}$:

$$\begin{aligned}
 P(q \in r \mid \mathcal{S}_r) &\propto K \sum_{k=1}^n \lambda_k \cdot c_{M_k}(q) \cdot \left(\frac{1}{K} \sum_{s \in \mathcal{S}_r} c_{M_k}(s) \right) \\
 &\propto \sum_{k=1}^n \lambda_k \cdot c_{M_k}(q) \cdot \mathbb{E}_{s \sim \mathcal{S}_r} [c_{M_k}(s)]
 \end{aligned} \tag{20}$$

This completes the proof. □

B More Experiments

B.1 Datasets

Transductive datasets (16). The transductive split contains graphs where test entities appear in the training graph. It includes FB15k-237 [43] and its sparse subsets (FB15k-237-10%, FB15k-237-20%, FB15k-237-50%), WN18RR [13], CoDEX-Small [37], CoDEX-Medium [37], CoDEX-Large [37], NELL-995 [30], ConceptNet100k [38], DBpedia100k [25], YAGO3-10 [40], AristoV4 [9], Hetionet [21], WDSinger [16], and NELL23k. The details for these datasets have been reported in Table 2

Inductive datasets — new entities, no new relations (18). These datasets introduce unseen entities at inference time while keeping the relation vocabulary fixed. They comprise the GraIL benchmark graphs [42]: FB15k-237-Inductive (v1–v4), WN18RR-Inductive (v1–v4), and NELL-Inductive (v1–v4); the ILPC 2022 graphs (small and large) [15]; and 4 INDIGO graphs [29, 20]: HM-1k, HM-3k, HM-5k, and HM-Indigo. The details for these datasets have been reported in Table 3.

Fully inductive datasets — new entities and new relations (23). These datasets require generalisation to both unseen entities and unseen relation types. They include the InGram graphs [24]: NL-Ingram (splits 0/25/50/75/100), FB-Ingram (25/50/75/100), and WK-Ingram (25/50/75/100); the MTDEA WikiTopics graphs [49]: WikiTopics-MT1 (health, tax), WikiTopics-MT2 (org, sci), WikiTopics-MT3 (art, infra), and WikiTopics-MT4 (sci, health); and two additional MTDEA graphs, Metafam and FBNEll. The details for these datasets have been reported in Table 4.

Table 3: 18 Inductive entity (e) datasets used in the experiments.

Dataset	Rels	Training Graph		Validation Graph			Test Graph		
		Entities	Triples	Entities	Triples	Valid	Entities	Triples	Test
FB v1	180	1594	4245	1594	4245	489	1093	1993	411
FB v2	200	2608	9739	2608	9739	1166	1660	4145	947
FB v3	215	3668	17986	3668	17986	2194	2501	7406	1731
FB v4	219	4707	27203	4707	27203	3352	3051	11714	2840
WN v1	9	2746	5410	2746	5410	630	922	1618	373
WN v2	10	6954	15262	6954	15262	1838	2757	4011	852
WN v3	11	12078	25901	12078	25901	3097	5084	6327	1143
WN v4	9	3861	7940	3861	7940	934	7084	12334	2823
NELL v1	14	3103	4687	3103	4687	414	225	833	201
NELL v2	88	2564	8219	2564	8219	922	2086	4586	935
NELL v3	142	4647	16393	4647	16393	1851	3566	8048	1620
NELL v4	76	2092	7546	2092	7546	876	2795	7073	1447
ILPC Small	48	10230	78616	6653	20960	2908	6653	20960	2902
ILPC Large	65	46626	202446	29246	77044	10179	29246	77044	10184
HM 1k	11	36237	93364	36311	93364	1771	9899	18638	476
HM 3k	11	32118	71097	32250	71097	1201	19218	38285	1349
HM 5k	11	28601	57601	28744	57601	900	23792	48425	2124
IndigoBM	229	12721	121601	12797	121601	14121	14775	250195	14904

Table 4: 23 Inductive entity and relation (e, r) datasets used in the experiments.

Dataset	Training Graph			Validation Graph				Test Graph			
	Entities	Rels	Triples	Entities	Rels	Triples	Valid	Entities	Rels	Triples	Test
FB-25	5190	163	91571	4097	216	17147	5716	4097	216	17147	5716
FB-50	5190	153	85375	4445	205	11636	3879	4445	205	11636	3879
FB-75	4659	134	62809	2792	186	9316	3106	2792	186	9316	3106
FB-100	4659	134	62809	2624	77	6987	2329	2624	77	6987	2329
WK-25	12659	47	41873	3228	74	3391	1130	3228	74	3391	1131
WK-50	12022	72	82481	9328	93	9672	3224	9328	93	9672	3225
WK-75	6853	52	28741	2722	65	3430	1143	2722	65	3430	1144
WK-100	9784	67	49875	12136	37	13487	4496	12136	37	13487	4496
NL-0	1814	134	7796	2026	112	2287	763	2026	112	2287	763
NL-25	4396	106	17578	2146	120	2230	743	2146	120	2230	744
NL-50	4396	106	17578	2335	119	2576	859	2335	119	2576	859
NL-75	2607	96	11058	1578	116	1818	606	1578	116	1818	607
NL-100	1258	55	7832	1709	53	2378	793	1709	53	2378	793
Metafam	1316	28	13821	1316	28	13821	590	656	28	7257	184
FBNEL	4636	100	10275	4636	100	10275	1055	4752	183	10685	597
Wiki MT1 tax	10000	10	17178	10000	10	17178	1908	10000	9	16526	1834
Wiki MT1 health	10000	7	14371	10000	7	14371	1596	10000	7	14110	1566
Wiki MT2 org	10000	10	23233	10000	10	23233	2581	10000	11	21976	2441
Wiki MT2 sci	10000	16	16471	10000	16	16471	1830	10000	16	14852	1650
Wiki MT3 art	10000	45	27262	10000	45	27262	3026	10000	45	28023	3113
Wiki MT3 infra	10000	24	21990	10000	24	21990	2443	10000	27	21646	2405
Wiki MT4 sci	10000	42	12576	10000	42	12576	1397	10000	42	12516	1388
Wiki MT4 health	10000	21	15539	10000	21	15539	1725	10000	20	15337	1703

B.2 More results

In this section, we show more detailed results of our methods. We compared the mrr performance of KGPFN with that of other advanced KG foundation models on 57 datasets. As shown in Fig. 5,

Fig. 6 and Fig. 7, KGPFN demonstrated competitive performance on most of the datasets. This demonstrates the advantage of in-context learning, where the model’s performance can be improved through the context without the need for additional training.

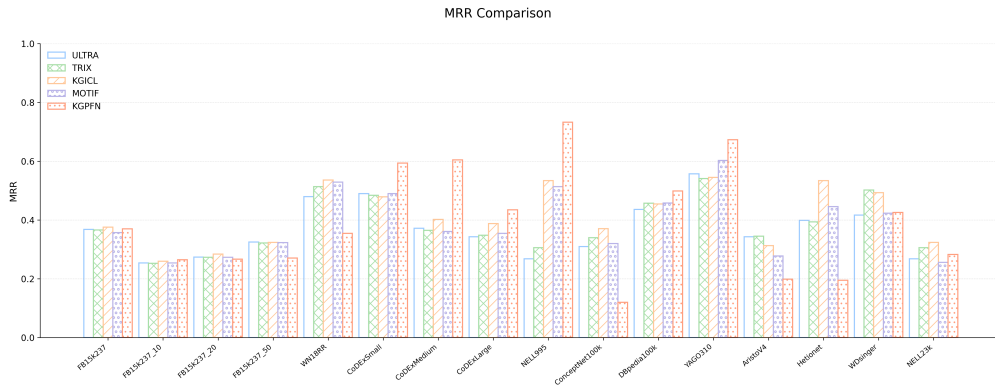


Figure 5: MRR on 16 transductive KGs.

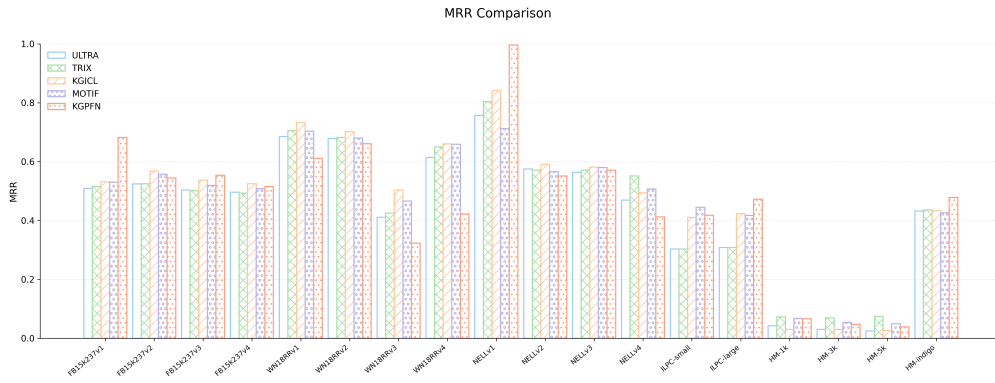


Figure 6: MRR on 18 inductive KGs.

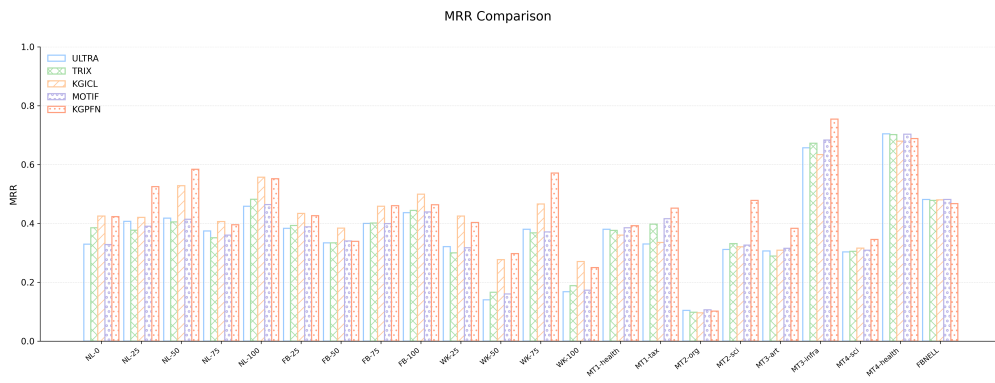


Figure 7: MRR on 23 full inductive KGs.

Here, we present the detailed performance of our model on each dataset and compare two PFN architectures, TabICL [34] and LIMIX [47], within our framework. For both architectures, we remove their original feature processing and encoding components, retaining only the feature-attention and sample-attention modules for context utilization. The results are reported in Tables 5, 6, and 7. As shown, the two architectures achieve comparable performance across different evaluation settings.

This suggests that the gains of our method mainly come from the proposed local/global context construction and the use of attention-based context aggregation, rather than from architecture-specific preprocessing or encoding designs. The consistent results also indicate that our framework is flexible and can accommodate different PFN variants for exploiting in-context support examples.

Table 5: Results on transductive datasets (MRR / Hits@10).

Dataset	KGPFN(TabICL)		KGPFN(LimiX)	
	MRR	Hits@10	MRR	Hits@10
FB15k237	0.370	0.586	0.389	0.586
FB15k237_10	0.265	0.453	0.275	0.453
FB15k237_20	0.267	0.421	0.281	0.445
FB15k237_50	0.271	0.390	0.297	0.438
WN18RR	0.355	0.590	0.399	0.547
CoDExSmall	0.594	0.859	0.592	0.828
CoDExMedium	0.605	0.828	0.641	0.820
CoDExLarge	0.435	0.781	0.494	0.750
NELL995	0.733	0.882	0.615	0.891
ConceptNet100k	0.120	0.312	0.092	0.148
DBpedia100k	0.499	0.805	0.526	0.813
YAGO310	0.673	0.836	0.716	0.836
AristoV4	0.199	0.422	0.272	0.523
Hetionet	0.195	0.360	0.228	0.375
WDSinger	0.426	0.562	0.412	0.539
NELL23k	0.283	0.516	0.301	0.555

Table 6: Results on inductive datasets (MRR / Hits@10).

Dataset	KGPFN(TabICL)		KGPFN(LimiX)	
	MRR	Hits@10	MRR	Hits@10
FB15k237v1	0.682	0.852	0.672	0.852
FB15k237v2	0.544	0.757	0.536	0.781
FB15k237v3	0.554	0.695	0.552	0.695
FB15k237v4	0.515	0.703	0.507	0.695
WN18RRv1	0.611	0.828	0.609	0.820
WN18RRv2	0.661	0.835	0.650	0.828
WN18RRv3	0.323	0.430	0.325	0.438
WN18RRv4	0.422	0.703	0.417	0.688
NELLv1	0.996	1.000	0.996	1.000
NELLv2	0.551	0.766	0.519	0.766
NELLv3	0.571	0.798	0.583	0.781
NELLv4	0.412	0.688	0.407	0.703
ILPC-small	0.472	0.710	0.410	0.695
ILPC-large	0.472	0.710	0.474	0.703
HM-1k	0.066	0.133	0.067	0.141
HM-3k	0.047	0.102	0.048	0.109
HM-5k	0.038	0.109	0.037	0.102
HM-indigo	0.478	0.703	0.476	0.695

Table 7: Results on full-inductive datasets (MRR / Hits@10).

Dataset	KGPFN(TabICL)		KGPFN(LimiX)	
	MRR	Hits@10	MRR	Hits@10
NL-0	0.423	0.625	0.385	0.586
NL-25	0.525	0.672	0.505	0.641
NL-50	0.584	0.727	0.553	0.719
NL-75	0.395	0.578	0.349	0.539
NL-100	0.552	0.704	0.535	0.695
FB-25	0.426	0.609	0.446	0.641
FB-50	0.339	0.594	0.334	0.602
FB-75	0.460	0.656	0.469	0.641
FB-100	0.463	0.688	0.475	0.711
WK-25	0.403	0.773	0.352	0.656
WK-50	0.297	0.539	0.307	0.508
WK-75	0.571	0.836	0.575	0.766
WK-100	0.250	0.516	0.293	0.492
MT1-health	0.392	0.609	0.464	0.617
MT1-tax	0.452	0.555	0.435	0.555
MT2-org	0.102	0.188	0.120	0.227
MT2-sci	0.478	0.648	0.483	0.633
MT3-art	0.383	0.625	0.439	0.648
MT3-infra	0.754	0.882	0.780	0.883
MT4-sci	0.345	0.593	0.351	0.594
MT4-health	0.688	0.789	0.738	0.813
Metafam	0.211	0.625	0.189	0.219
FBNELL	0.467	0.664	0.449	0.672

C Limitation

Due to the limitation of computing resources, our model lacks the verification of the scaling law on knowledge graph tasks.

D Broader Impact

This paper aims to advance the field of knowledge graph foundation models. Our work contributes to the field of Machine Learning and has many potential societal consequences. It may play an important role in understanding fields such as neural graph database and recommendation systems based on knowledge graphs. However, we believe that there are no negative impacts that need clarification.